

High-dimensional GARCH process segmentation with an application to Value-at-Risk

Haeran Cho

School of Mathematics, University of Bristol

and

Karolos K. Korkas

Citigroup

December 14, 2024

Abstract

An assumption in modelling financial risk is that the underlying asset returns are stationary. However, there is now strong evidence that multivariate financial time series entail changes not only in their within-series dependence structure, but also in the correlations among them. Failing to address these structural changes is more likely to result in a crude approximation of the risk measures adopted and, thereby, to affect the monitoring and managing capital adequacy of financial institutions. For this reason, we propose a method for consistent detection of multiple change-points in (possibly high) N -dimensional GARCH panel data set, where both individual GARCH processes and their correlations are allowed to change. The method consists of two stages: i) the transformation of N -dimensional GARCH processes into $N(N + 1)/2$ -‘mean plus noise’ series, and ii) the application of the Double CUSUM Binary Segmentation algorithm for simultaneous segmentation of the $N(N + 1)/2$ -dimensional transformation of the input data. We show the consistency of the proposed methodology in estimating both the total number and locations of the change-points. Its good performance is demonstrated through an extensive simulation study and an application to a real dataset, where we show the importance of identifying the change-points prior to calculating Value-at-Risk under a stressed scenario.

Key words and phrases: Double CUSUM Binary Segmentation, GARCH, high dimensionality, multiple change-point detection, multivariate risk, nonstationarity

1 Introduction

The increased financial uncertainty during the recent economic crisis has confirmed the strong volatility linkage between asset markets. For example, there is now strong evidence that the economy and oil prices ([Hamilton, 2003](#)), foreign exchange rates ([Baillie, 1991](#)), equity markets ([Baele, 2003](#)) and crude oil and agricultural commodities ([Du et al., 2011](#)) are related – a phenomenon commonly referred to as volatility spillover. Such behavior is naturally expected since the rate of information influences the volatility in asset returns and therefore, the information flow from one asset market can be incorporated into another related market ([Ross, 1989](#)).

Motivated by such observations, joint modelling of several financial returns has attracted considerable attention in the literature, and many models have been proposed for multivariate GARCH processes including the vectorized multivariate GARCH models ([Bollerslev et al., 1988](#)), the Baba-Engle-Kraft-Kroner (BEKK) model ([Engle and Kroner, 1995](#)), the constant conditional correlation (CCC) model ([Bollerslev, 1990](#)), the dynamic conditional correlation (DCC) model ([Engle, 2002](#)), the generalized orthogonal GARCH models ([Van der Weide, 2002](#)), the full-factor multivariate GARCH models ([Vrontos et al., 2003](#)) and the conditionally uncorrelated components-based multivariate volatility processes ([Fan et al., 2008](#)); for a survey of recent approaches to multivariate GARCH modelling and inference, see [Bauwens et al. \(2006\)](#).

The assumption that the underlying dynamics remain unchanged is rather restrictive considering that the fundamentals driving an economy, or the asset markets in particular, exhibit sudden changes or regimes switches. These change-points (a.k.a. structural breaks or break-points) in various economic and financial time series are well documented, see [Hansen \(2001\)](#) and [Stock and Watson \(2002\)](#) among many others. [Pesaran and Timmermann \(2007\)](#) examined eight major currency pairs and established that stationary volatility modelling induces an upward bias in the mean square forecast error when change-points exist in the exchange rate volatility. Failing to account for structural breaks, exchange rate volatility is found close to be integrated. [Cappiello et al. \(2006\)](#) documented a change-point in the correlation between international equity and bond returns after the introduction of the euro currency, supporting the need for a method that accounts for change-points in both the conditional volatility and correlation. [Ewing and Malik \(2013\)](#) found a significant transmission of volatility (spillover) between oil and gold when change-points in variance were considered, compared to a weaker

transmission when change-points are ignored. [Diebold and Inoue \(2001\)](#) noted that stochastic regime switching may be confused with long memory and the presence of structural breaks may easily be regarded as fractional integration. In [Mikosch and Střaricř \(2004\)](#), a theoretical basis is provided for accounting for the long-range dependence in volatility and the integrated GARCH effect in long log-return series, by assuming that the series undergoes changes in unconditional mean or variance.

Investigations into the tests for a *single* structural break in univariate, ARCH-type models have been made in [Kokoszka and Leipus \(2000\)](#), [Kokoszka and Teyssiře \(2002\)](#), [Lee et al. \(2003\)](#), [Berkes et al. \(2004\)](#) and [De Pooter and Van Dijk \(2004\)](#). [Fryzlewicz and Subba Rao \(2014\)](#) developed a two-stage procedure termed BASTA (binary segmentation for transformed ARCH), for detecting multiple change-points in the parameters involved in modelling the conditional variance of univariate series. [Andreou and Ghysels \(2003\)](#) studied change-point detection in the co-movement of a pair of returns, by examining the product of returns standardized via data-driven volatility filters. For modelling multivariate, possibly high-dimensional data such as asset portfolios consisting of hundreds of different assets, the aforementioned change-point detection methods may be repeatedly applied to individual and pairs of component series. However, identification of the common change-points becomes challenging even for data of moderately high dimensions, due to the bias present in the change-points estimated from each application. Besides, such an approach does not fully exploit the fact that a change-point may be shared cross-sectionally, and therefore loss of power in change-point detection cannot be ruled out.

In this paper, we propose to address the need for multiple change-point detection in multivariate, possibly high-dimensional GARCH processes where both within-series and cross-correlation structure may undergo changes. Simultaneous segmentation of high-dimensional GARCH processes is achieved via two-stage procedure in line with [Fryzlewicz and Subba Rao \(2014\)](#) and [Andreou and Ghysels \(2003\)](#). Firstly, the N GARCH processes are transformed into $N(N+1)/2$ sequences based on empirical residual series and their cross-products, whereby change-points are detectable from the means of the transformed series. The collection of transformed series serves as an input to the second stage, which adopts the Double CUSUM Binary Segmentation algorithm proposed in [Cho \(2016\)](#) for multiple change-point detection in generic additive, high-dimensional panel data. We show the consistency of the two-stage methodology in estimating both the total number and locations of the multiple change-points.

The rest of the paper is organized as follows. In [Section 2](#), we introduce a time-varying

multivariate GARCH model which provides a framework for the theoretical treatment of our methodology. Section 3 is devoted to the description of the proposed two-stage methodology. Its finite sample performance is investigated on sets of simulated data in Section 4. In Section 5, we apply our method on a real financial data set and validate its performance by showing the importance of knowing the change-points in a portfolio of assets in risk management. Section 6 concludes the paper. All the proofs are provided in the supplementary document.

2 Time-varying multivariate GARCH model

We consider the following time-varying multivariate GARCH (tv-MGARCH) model denoted by $\mathbf{r}_t = (r_{1,t}, \dots, r_{N,t})^\top$, $t = 1, \dots, T$:

$$r_{i,t} = \sqrt{h_{i,t}} \varepsilon_{i,t} \quad \text{with } \boldsymbol{\varepsilon}_t = (\varepsilon_{1,t}, \dots, \varepsilon_{N,t})^\top \sim (\mathbf{0}, \Sigma(t)), \quad \text{and} \quad (1)$$

$$h_{i,t} = \omega_i(t) + \sum_{j=1}^p \alpha_{i,j}(t) r_{i,t-j}^2 + \sum_{k=1}^q \beta_{i,k}(t) h_{i,t-k}. \quad (2)$$

The time-varying covariance matrix of the independent random innovations $\boldsymbol{\varepsilon}_t$ satisfies $\text{var}(\boldsymbol{\varepsilon}_t) = \Sigma(t) = [\sigma_{i,i'}(t)]_{i,i'=1}^N$ with $\sigma_{i,i}(t) = 1$ for all i and t . We denote the vector of parameters involved in modelling the within-panel conditional variance of $r_{i,t}$ by

$$\boldsymbol{\Omega}_i(t) = (\omega_i(t), \alpha_{i,1}(t), \dots, \alpha_{i,p}(t), \beta_{i,1}(t), \dots, \beta_{i,q}(t))^\top \in \mathbb{R}^{1+p+q},$$

and that involved in modelling the cross-correlations of $\varepsilon_{i,t}$ by

$$\boldsymbol{\Theta}_i(t) = (\sigma_{i,1}(t), \dots, \sigma_{i,i-1}(t), \sigma_{i,i+1}(t), \dots, \sigma_{i,N}(t))^\top \in \mathbb{R}^{N-1}.$$

Then, $\boldsymbol{\Omega}_i(t)$ and $\boldsymbol{\Theta}_i(t)$ are piecewise constant in t and share B change-points $0 \equiv \eta_0 < \eta_1 < \dots < \eta_B < \eta_{B+1} \equiv T$ across $i = 1, \dots, N$, in the sense that at any η_b , either $\boldsymbol{\Omega}_i(\eta_b) \neq \boldsymbol{\Omega}_i(\eta_b + 1)$ or $\boldsymbol{\Theta}_i(\eta_b) \neq \boldsymbol{\Theta}_i(\eta_b + 1)$ and $\boldsymbol{\Omega}_i(t) = \boldsymbol{\Omega}_i(t + 1)$ and $\boldsymbol{\Theta}_i(t) = \boldsymbol{\Theta}_i(t + 1)$ for all $t \neq \eta_b$.

In (1)–(2), we assume that the (unconditional) correlations across the components of \mathbf{r}_t are attributed to the correlations of $\boldsymbol{\varepsilon}_t$, and that the conditional variance within each component series is modelled separately as in the standard univariate GARCH processes. Thus, the tv-MGARCH model is reduced to the CCC model of [Bollerslev \(1990\)](#) over each stationary segment $[\eta_b + 1, \eta_{b+1}]$, i.e., $\mathbb{E}(h_{i,t}^{-1/2} r_{i,t} h_{i',t}^{-1/2} r_{i',t} | \mathcal{F}_{t-1}) = \sigma_{i,i'}(\eta_b + 1)$, where \mathcal{F}_{t-1} denotes the

σ -algebra $\sigma\{\mathbf{r}_s, s \leq t-1\}$. We take this approach with the aim of specifying the parameters to which structural changes may be introduced, rather than in order to actually model the conditional correlation between pairs of component series; it can be accomplished once the structural change-points are estimated and (approximately) stationary segments are identified. We note that the multivariate GARCH processes literature, as those cited in Introduction, considers a relatively lower-dimensional applications ($N \leq 8$), whereas we consider GARCH modelling of both simulated and real datasets of higher dimensions ($N \geq 31$) in this paper.

We assume the following conditions on (1)–(2).

(A1) The dimensionality N satisfies $N \sim T^\theta$ for some $\theta \in [0, \infty)$.

(A2) For some $\epsilon_1 > 0$, $\Xi_1 < \infty$ and all T , we have

$$\min_{1 \leq i \leq N} \inf_{t \in \mathbb{Z}} \omega_i(t) > \epsilon_1 \text{ and } \max_{1 \leq i \leq N} \inf_{t \in \mathbb{Z}} \omega_i(t) \leq \Xi_1 < \infty.$$

(A3) For some $\epsilon_2 \in (0, 1)$ and all T , we have

$$\max_{1 \leq i \leq N} \inf_{t \in \mathbb{Z}} \left\{ \sum_{j=1}^p \alpha_{i,j}(t) + \sum_{k=1}^q \beta_{i,k}(t) \right\} \leq 1 - \epsilon_2.$$

Assumption (A1) indicates that the dimensionality can either be fixed or increase with T at a polynomial rate. Assumptions (A2)–(A3) guarantee that between any two consecutive change-points, each $r_{i,t}$ admits a well-defined solution a.s.

For a non-stationary stochastic process X_t , its strong-mixing rate is defined as a sequence of coefficients

$$\alpha(k) = \sup_{t \in \mathbb{Z}} \sup_{\substack{G \in \sigma(X_{t+k}, X_{t+k+1}, \dots), \\ H \in \sigma(X_t, X_{t-1}, \dots)}} |\mathbb{P}(G \cap H) - \mathbb{P}(G)\mathbb{P}(H)|.$$

For BEKK multivariate GARCH models introduced in [Engle and Kroner \(1995\)](#), Theorem 2.4 of [Boussama et al. \(2011\)](#) shows that there exists a unique and strictly stationary solution, which is geometrically β -mixing and hence also strong mixing, i.e., $\alpha(k) \rightarrow 0$ as $k \rightarrow \infty$ with $\alpha(k) \sim \alpha^k$ for some $\alpha \in (0, 1)$. Adopting the theoretical tools developed in [Fryzlewicz and Subba Rao \(2011\)](#), where the mixing rate of univariate, time-varying ARCH processes was investigated, we establish that any pair of time-varying GARCH processes $\mathbf{r}_{ii',t} = (r_{i,t}, r_{i',t})^\top$,

$1 \leq i < i' \leq N$, is strong mixing at a geometric rate. In order to achieve this goal, the following Lipschitz-type condition is imposed on the joint density of $(\varepsilon_{i,t}^2, \varepsilon_{i',t}^2)^\top$. We adopt the notations \vee and \wedge to denote $a \vee b = \max(a, b)$ and $a \wedge b = \min(a, b)$.

(A4) The joint distribution of $\varepsilon_{i,t}^2$ and $\varepsilon_{i',t}^2$, denoted by $f_{i,i'}(u, v)$, satisfies the following: for any $a > 0$, there exists fixed $K > 0$ independent of a such that

$$\left\{ \int \int |f_{i,i'}(u, v) - f_{i,i'}(u(1+a), v)| dudv \right\} \vee \left\{ \int \int |f_{i,i'}(u, v) - f_{i,i'}(u, v(1+a))| dudv \right\} \leq Ka$$

uniformly over $i, i' = 1, \dots, N, i \neq i'$.

Then, time-varying bivariate GARCH processes $\mathbf{r}_{ii',t}$, $i < i'$, is strong mixing as below (see Appendix A.4 in the supplementary document for the proof).

Proposition 1. Under (A2)–(A4), there exists some $\alpha \in (0, 1)$ such that

$$\sup_{1 \leq i < i' \leq N} \sup_{\substack{G \in \sigma(\mathbf{r}_{i,i',u}: u \geq t+k), \\ H \in \sigma(\mathbf{r}_{i,i',u}: u \leq t)}} |\mathbb{P}(G \cap H) - \mathbb{P}(G)\mathbb{P}(H)| \leq M\alpha^k,$$

where M is a finite constant independent of t and k .

3 Two-stage change-point detection methodology

3.1 Stage 1: Transformation of GARCH processes

Empirical residuals have been widely adopted for detecting changes in the unconditional variance and/or parameters of univariate, conditionally heteroscedastic processes, see [Kokoszka and Teyssière \(2002\)](#), [Lee et al. \(2003\)](#), [De Pooter and Van Dijk \(2004\)](#) and [Fryzlewicz and Subba Rao \(2014\)](#). For stationary processes, the squared empirical residuals may be regarded as approximating a series of i.i.d. random variables. Even in the presence of change-points, such transformation tends to reduce the autocorrelations in the transformed series to a considerable degree, while the change-points are reflected in their means.

For the segmentation of tv-MGARCH processes defined in Section 2, we propose to transform \mathbf{r}_t into $d \equiv d_N = N(N+1)/2$ series such that a change in any of $\boldsymbol{\Omega}_i(t)$ or $\boldsymbol{\Theta}_i(t)$ for all $i = 1, \dots, n$, are detectable as a change-point in the mean of at least one out of the

d transformed series. We first transform the N processes $r_{i,t}$ individually using a function $g_1 : \mathbb{R}^{1+p+q} \rightarrow \mathbb{R}$, which takes $\mathbf{r}_{i,t}^{t-p} = (r_{i,t}, \dots, r_{i,t-p})^\top$ and $\mathbf{h}_{i,t-1}^{t-q} = (h_{i,t-1}, \dots, h_{i,t-q})^\top$ as an input. We require that g_1 is bounded and Lipschitz continuous.

(A5) The function $g_1 : \mathbb{R}^{1+p+q} \rightarrow \mathbb{R}$ satisfies $|g_1| \leq \bar{g} < \infty$ and is Lipschitz continuous in its squared arguments, i.e., $|g_1(z_0, \dots, z_{p+q}) - g_1(z'_0, \dots, z'_{p+q})| \leq C_g \sum_{k=0}^{p+q} |z_k^2 - (z'_k)^2|$.

Motivated by the univariate methods based on empirical residuals including BASTA-res (Fryzlewicz and Subba Rao, 2014), we select g_1 such that

$$\begin{aligned} U_{i,t} &= g_1(\mathbf{r}_{i,t}^{t-p}, \mathbf{h}_{i,t-1}^{t-q}) = \frac{r_{i,t}^2}{\check{h}_{i,t}}, \quad \text{where} \\ \check{h}_{i,t} &= C_{i,0} + \sum_{j=1}^p C_{i,j} r_{i,t-j}^2 + \sum_{k=1}^q C_{i,p+k} h_{i,t-k} + \epsilon r_{i,t}^2. \end{aligned} \quad (3)$$

Following Fryzlewicz and Subba Rao (2014), we add ϵX_t^2 to $\check{h}_{i,t}$ in order to ensure the boundedness of U_t with an arbitrary small positive constant ϵ . When any parameter in $\boldsymbol{\Omega}_i(t)$ undergoes a shift over time, this change is expected to be reflected as a shift in $\mathbb{E}(U_{i,t})$. More specifically,

$$U_{i,t} = \frac{h_{i,t}}{\check{h}_{i,t}} \cdot \frac{r_{i,t}^2}{h_{i,t}} = \frac{h_{i,t}}{\check{h}_{i,t}} \varepsilon_{i,t}^2 = \frac{h_{i,t}}{\check{h}_{i,t}} + \frac{h_{i,t}}{\check{h}_{i,t}} (\varepsilon_{i,t}^2 - 1), \quad (4)$$

so that $\mathbb{E}(U_{i,t}) = \mathbb{E}(h_{i,t}/\check{h}_{i,t})$ contains any change in $\boldsymbol{\Omega}_i(t)$ as a change in its value. Choices of the parameters $C_{i,j}$, $j = 0, \dots, p+q$ and the treatment of (unobservables) $h_{i,t}$ are discussed in Section 3.3.

To capture any changes in the cross-sectional dependence structure of \mathbf{r}_t or, more precisely, in any $\sigma_{i,i'}(t)$ for $i \neq i'$, we select the function $g_2 : \mathbb{R}^{2+2p+2q} \rightarrow \mathbb{R}$:

$$U_{ii',t} = g_2(\mathbf{r}_{i,t}^{t-p}, \mathbf{h}_{i,t-1}^{t-q}, \mathbf{r}_{i',t}^{t-p}, \mathbf{h}_{i',t-1}^{t-q}) = (U_{i,t}^{1/2} - s_{i,i'} U_{i',t}^{1/2})^2$$

where $s_{i,i'} \in \{1, -1\}$ and, with a slight abuse of notation, we define

$$U_{i,t}^{1/2} = g_3(\mathbf{r}_{i,t}^{t-p}, \mathbf{h}_{i,t-1}^{t-q}) = \frac{r_{i,t}}{\sqrt{\check{h}_{i,t}}},$$

so that the sign of $r_{i,t}$ is preserved as the sign of $U_{i,t}^{1/2}$. When g_1 meets the requirements in (A5), g_2 is also bounded and Lipschitz continuous in its squared arguments (see Appendix

A.3 of the supplementary document). Similarly as in (4), $U_{ii',t}$ is decomposed as

$$\begin{aligned} U_{ii',t} &= \left(\sqrt{\frac{h_{i,t}}{\bar{h}_{i,t}}} \frac{r_{i,t}}{\sqrt{h_{i,t}}} - s_{i,i'} \sqrt{\frac{h_{i',t}}{\bar{h}_{i',t}}} \frac{r_{i',t}}{\sqrt{h_{i',t}}} \right)^2 = \frac{h_{i,t}}{\bar{h}_{i,t}} \varepsilon_{i,t}^2 + \frac{h_{i',t}}{\bar{h}_{i',t}} \varepsilon_{i',t}^2 - 2s_{i,i'} \sqrt{\frac{h_{i,t}h_{i',t}}{\bar{h}_{i,t}\bar{h}_{i',t}}} \varepsilon_{i,t}\varepsilon_{i',t} \\ &= \frac{h_{i,t}}{\bar{h}_{i,t}} + \frac{h_{i,t}}{\bar{h}_{i,t}} (\varepsilon_{i,t}^2 - 1) + \frac{h_{i',t}}{\bar{h}_{i',t}} + \frac{h_{i',t}}{\bar{h}_{i',t}} (\varepsilon_{i',t}^2 - 1) - 2s_{i,i'} \sqrt{\frac{h_{i,t}h_{i',t}}{\bar{h}_{i,t}\bar{h}_{i',t}}} \{\sigma_{i,i'}(t) + \varepsilon_{i,t}\varepsilon_{i',t} - \sigma_{i,i'}(t)\}, \end{aligned}$$

such that $\mathbb{E}(U_{ii',t})$ contains any change in $\sigma_{i,i'}(t)$ as a change in its value.

By regarding $U_{i,t}$ as empirical residuals obtained by applying volatility filters, [Andreou and Ghysels \(2003\)](#) proposed to search for structural changes in the co-movement of a pair of series $(r_{1,t}, r_{2,t})^\top$ by examining $U_{1,t}^{1/2}U_{2,t}^{1/2}$, $U_{1,t}U_{2,t}$ and $|U_{1,t}^{1/2}U_{2,t}^{1/2}|$. Instead, we adopt $U_{ii',t}$. Its formulation is motivated by the observation made in [Cho and Fryzlewicz \(2015\)](#): for given $\{a_t\}$ and $\{b_t\}$, any changes in $\mathbb{E}(a_t^2)$, $\mathbb{E}(b_t^2)$ and $\mathbb{E}(a_t b_t)$ are detectable by jointly examining $\mathbb{E}(a_t^2)$, $\mathbb{E}(b_t^2)$ and $\mathbb{E}\{(a_t - s_{a,b}b_t)^2\}$ for any $s_{a,b} \in \{1, -1\}$ regardless of its choice. We provide a guide on the empirical choice of $s_{i,i'}$ in Section 3.3.

In addition, we can regard $U_{ii',t}$ on an equal footing with $U_{i,t}$ and $U_{i',t}$, which is essential in accomplishing the simultaneous segmentation of \mathbf{r}_t according to both within-series and cross-sectional dependence structure. Under the stationarity, the choice of $C_{i,0} = \omega_i$, $C_{i,j} = \alpha_{i,j}$ and $C_{i,p+k} = \beta_{i,k}$ leads to $U_{i,t}$ approximating $\varepsilon_{i,t}^2$, while $U_{ii',t}$ approximates $(\varepsilon_{i,t} - s_{i,i'}\varepsilon_{i',t})^2$. Upon further imposing Gaussianity on $\varepsilon_{i,t}$, all $U_{i,t}$ and $U_{ii',t}$ follow a scaled χ_1^2 distribution. Note that the same arguments do not apply to $U_{i,t}^{1/2}U_{i',t}^{1/2}$ or other transformations studied in [Andreou and Ghysels \(2003\)](#).

In summary, we propose to detect any changes in $\boldsymbol{\Omega}_i(t)$ and $\boldsymbol{\Theta}_i(t)$, $i = 1, \dots, N$ simultaneously from the d -dimensional transformation of \mathbf{r}_t :

$$\{U_{i,t}, 1 \leq i \leq N; U_{ii',t}, 1 \leq i < i' \leq N; 1 \leq t \leq T\}, \quad (5)$$

which serves as an input to the high-dimensional change-point detection algorithm we introduce in the next section.

Let $\{\mathbf{r}_{i,t}^b\}_{t=1}^T$ denote a stationary multivariate GARCH(p, q) process which follows (1)–(2) with the fixed parameters associated with the stationary segment $[\eta_b + 1, \eta_{b+1}]$, and the identical innovation $\boldsymbol{\varepsilon}_t$ that has constant covariance matrix over $[\eta_b + 1, \eta_{b+1}]$. For each b , we form the processes $\tilde{U}_{i,t}^b = g_1(\mathbf{r}_{i,t}^{b,t-p}, \mathbf{h}_{i,t-1}^{b,t-q})$ and $\tilde{U}_{ii',t}^b = g_2(\mathbf{r}_{i,t}^{b,t-p}, \mathbf{h}_{i,t-1}^{b,t-q}, \mathbf{r}_{i',t}^{b,t-p}, \mathbf{h}_{i',t-1}^{b,t-q})$. Besides, denoting the index of the change-point strictly to the left of and nearest to t by

$v(t) = \max\{0 \leq b \leq B : \eta_b < t\}$, we define $\tilde{g}_{i,t} = \mathbb{E}(\tilde{U}_{i,t}^{v(t)})$ and $\tilde{g}_{ii',t} = \mathbb{E}(\tilde{U}_{ii',t}^{v(t)})$. Unlike $\mathbb{E}(U_{i,t})$ or $\mathbb{E}(U_{ii',t})$, thus-generated $\tilde{g}_{i,t}$ and $\tilde{g}_{ii',t}$ are *exactly* constant between any two adjacent change-points.

Then, denoting each generic element of the input data in (5) by $x_{j,t}$ (with $j = (N-i/2)(i-1) + i'$ and $U_{ii,t} \equiv U_{i,t}$ for notational convenience), it admits the decomposition

$$x_{j,t} = f_{j,t} + z_{j,t}, \quad 1 \leq j \leq d; \quad 1 \leq t \leq T, \quad (6)$$

where $f_{j,t} = \tilde{g}_{ii',t}$ (with $\tilde{g}_{ii,t} \equiv \tilde{g}_{i,t}$) are piecewise constant signals sharing the B change-points in $\Omega_i(t)$ and $\Theta_i(t)$ for all $i = 1, \dots, N$. In other words, at each η_b , there exists at least a single j for which $f_{j,\eta_{b+1}} - f_{j,\eta_b} \neq 0$, and $f_{j,t+1} - f_{j,t} = 0$ for all j when $t \neq \eta_b$, $1 \leq b \leq B$. By its construction, $z_{j,t} = U_{ii',t} - \tilde{U}_{ii',t}^{v(t)}$ does not satisfy $\mathbb{E}(z_{j,t}) = 0$ but, due to the mixing properties of $U_{ii',t}$ given in Proposition 1, its partial sums can be bounded by a term logarithmic in T .

Lemma 1. Let (A1)–(A5) hold. Defining the set $\mathcal{I}_1 = \{(s, e) : 1 \leq s < e \leq T\}$ and the event

$$\mathcal{E}_1 = \left\{ \max_{1 \leq j \leq d} \max_{(s,e) \in \mathcal{I}_1} \frac{1}{\sqrt{e-s+1}} \left| \sum_{t=s}^e z_{j,t} \right| \leq c_2 \log^\varpi T \right\}$$

with some fixed $\varpi > 1$, we have $\mathbb{P}(\mathcal{E}_1) \rightarrow 1$ as $T \rightarrow \infty$.

3.2 Stage 2: Binary segmentation for tv-MGARCH processes

In this section, we introduce the second stage of the proposed methodology that segments the d -dimensional transformation of \mathbf{r}_t , using the notations given below the additive model in (6).

3.2.1 Double CUSUM binary segmentation

Cumulative sum (CUSUM) statistics have been widely adopted for change-point detection in both univariate and multivariate data. A series of CUSUM statistics computed on $x_{j,t}$ over a generic segment $[s, e]$ for some $1 \leq s < e \leq T$, is defined as

$$\mathcal{X}_{s,c,e}^j = \sqrt{\frac{(c-s+1)(e-c)}{e-s+1}} \left(\frac{1}{c-s+1} \sum_{t=s}^c x_{j,t} - \frac{1}{e-c} \sum_{t=c+1}^e x_{j,t} \right), \quad c = s, \dots, e-1.$$

Combined with the binary segmentation algorithm, the CUSUM statistic has been frequently adopted to segment univariate data; see [Vostrikova \(1981\)](#) and [Venkatraman \(1992\)](#) for the

theoretical treatment of its application to the canonical additive model with independent noise, and [Fryzlewicz and Subba Rao \(2014\)](#) for its application to segment time-varying ARCH processes.

For change-point detection in multivariate data, we may apply change-point detection procedures for univariate data to each $x_{j,t}$ separately as suggested by [Andreou and Ghysels \(2003\)](#), and then prune down the estimated change-points cross-sectionally. However, identification of common change-points is a challenging task even for moderately large d . Moreover, such an approach does not exploit the cross-sectional structure of the change-points that may be shared by multiple coordinates. The importance of simultaneous change-point analysis in high-dimensional data has been recognised in recent years, and several methods have been proposed which are based on aggregating high-dimensional CUSUM series $\mathcal{X}_{1,c,T}^j$, typically by taking their point-wise maximum (referred to as MAX throughout the paper) or average (AVG); see [Groen et al. \(2013\)](#), [Horváth and Hušková \(2012\)](#) and [Jirak \(2015\)](#) for their details.

We adopt the Double CUSUM Binary Segmentation (DCBS) algorithm proposed in [Cho \(2016\)](#) for multiple change-point detection in $x_{j,t}$ via high-dimensional CUSUM series aggregation. The majority of the literature in change-point analysis, including the references given in Introduction and above, concerns the problem of single change-point detection and may not easily be extended to multiple change-point scenarios. The DCBS algorithm (a) guarantees the consistency in multiple change-point detection in high-dimensional settings that allow the cross-sectional size of change to decrease with increasing sample size (see Assumption (B4) in Section 3.2.2), and (b) admits both serial- and cross-correlations in the data, which is a case highly relevant to the time series data considered in this paper.

The Double CUSUM (DC) operator takes the CUSUM series $\mathcal{X}_{s,c,e}^j$ and returns a two-dimensional array of DC statistics:

$$\mathcal{D}_{s,c,e}(n) = \sqrt{\frac{n(2d-n)}{2d}} \left(\frac{1}{n} \sum_{j=1}^n |\mathcal{X}_{s,c,e}^{(j)}| - \frac{1}{2d-n} \sum_{j=n+1}^d |\mathcal{X}_{s,c,e}^{(j)}| \right) \quad (7)$$

for $c = s, \dots, e-1$ and $n = 1, \dots, d$, where $|\mathcal{X}_{s,c,e}^{(j)}|$ denote the ordered CUSUM values at each c such that $|\mathcal{X}_{s,c,e}^{(1)}| \geq |\mathcal{X}_{s,c,e}^{(2)}| \geq \dots \geq |\mathcal{X}_{s,c,e}^{(d)}|$. Then, the test statistic is derived by maximising the two-dimensional array over both time and cross-sectional indices, as

$$\mathcal{T}_{s,e} = \max_{c \in [s,e]} \max_{1 \leq n \leq d} \mathcal{D}_{s,c,e}(n), \quad (8)$$

which is compared against a threshold $\pi_{d,T}$ for determining the presence of a change-point over the interval $[s, e]$. If $\mathcal{T}_{s,e} > \pi_{d,T}$, the location of the change-point is identified as

$$\hat{\eta} = \arg \max_{c \in [s,e]} \max_{1 \leq n \leq d} \mathcal{D}_{s,c,e}(n).$$

The Double CUSUM Binary Segmentation (DCBS) algorithm is formulated as below, The index l is used to denote the level (indicating the progression of the segmentation procedure) and m to denote the location of the node at each level in the binary tree grown by the DCBS algorithm.

The double CUSUM Binary Segmentation algorithm

Step 0 Set $(l, m) = (1, 1)$, $s_{l,m} = 1$ and $e_{l,m} = T$.

Step 1 At the current level l , repeat the following for all m .

Step 1.1 Letting $s = s_{l,m}$ and $e = e_{l,m}$, obtain the series of CUSUMs $\mathcal{X}_{s,c,e}^j$ for $c \in [s, e]$ and $j = 1, \dots, d$, on which $\mathcal{D}_{s,c,e}(n)$ is computed over all c and $n \in \{1, \dots, d\}$.

Step 1.2 Obtain the test statistic $\mathcal{T}_{s,e} = \max_{c \in [s,e]} \max_{1 \leq n \leq d} \mathcal{D}_{s,c,e}(n)$.

Step 1.3 If $\mathcal{T}_{s,e} \leq \pi_{d,T}$, quit searching for change-points on the interval $[s, e]$.

On the other hand, if $\mathcal{T}_{s,e} > \pi_{d,T}$, identify $\hat{\eta} = \arg \max_{c \in [s,e]} \max_{1 \leq n \leq d} \mathcal{D}_{s,c,e}(n)$ and proceed to Step 1.4.

Step 1.4 Add $\hat{\eta}$ to the set of estimated change-points and divide the interval $[s_{l,m}, e_{l,m}]$ into two sub-intervals $[s_{l+1,2m-1}, e_{l+1,2m-1}]$ and $[s_{l+1,2m}, e_{l+1,2m}]$, where $s_{l+1,2m-1} = s_{l,m}$, $e_{l+1,2m-1} = \hat{\eta}$, $s_{l+1,2m} = \hat{\eta} + 1$ and $e_{l+1,2m} = e_{l,m}$.

Step 2 Once $[s_{l,m}, e_{l,m}]$ for all m are examined at level l , set $l \leftarrow l + 1$ and go to Step 1.

Step 1.3 furnishes with a stopping rule to the DCBS algorithm; the search for further change-points is terminated once $\mathcal{T}_{s,e} \leq \pi_{d,T}$ on every segment $[s, e]$ defined by two adjacent estimated change-points.

3.2.2 Theoretical properties of DCBS algorithm

From the definition of $\tilde{g}_{i,t}$ and $\tilde{g}_{i',t}$, piecewise constant signals $\{f_{j,t}\}_{t=1}^T$, $j = 1, \dots, d$ contain the B change-points η_b , $b = 1, \dots, B$ shared by the vectors of piecewise constant parameters

$\Omega_i(t)$ and $\Theta_i(t)$, $i = 1, \dots, N$. In other words, at each change-point η_b , there exists an index set $\Pi_b = \{1 \leq j \leq d : \Delta_{j,b} = |f_{j,\eta_{b+1}} - f_{j,\eta_b}| > 0\} \subset \{1, \dots, d\}$ with its cardinality satisfying $m_b = |\Pi_b| \geq 1$. In order to establish the theoretical consistency of the DCBS algorithm, we impose the following conditions chiefly on the quantities that control the detectability of each change-point η_b .

- (B1) There exists a fixed constant $\bar{f} > 0$ such that $\max_{1 \leq j \leq d} \max_{1 \leq t \leq T} |f_{j,t}| \leq \bar{f}$.
- (B2) There exists a fixed constant $c_1 > 0$ such that $\min_{0 \leq b \leq B} (\eta_{b+1} - \eta_b) \geq c_1 T^\gamma$ for some $\gamma \in (6/7, 1]$ (with $\eta_0 = 0$ and $\eta_{B+1} = T$).
- (B3) The number of change-points, B , is unknown and satisfies $B \leq \log^\vartheta T$ for some fixed $\vartheta > 0$.
- (B4) At each η_b , let $\tilde{\Delta}_b = m_b^{-1} \sum_{j \in \Pi_b} \Delta_{j,b}$. Then, we have $\underline{\Delta}_{d,T} = \min_{1 \leq b \leq B} m_b^{1/2} \tilde{\Delta}_b$ satisfy $(d^{1/2} \log T)^{-1} T^{7\gamma/4 - 3/2} \underline{\Delta}_{d,T} \rightarrow \infty$ as $T \rightarrow \infty$.

The condition in (B1) holds trivially as a consequence of (A5). In general, change-point detection becomes more challenging as the distance between two adjacent change-points decreases. This is reflected on (B2), which still allows the case where $T^{-1}(\eta_{b+1} - \eta_b) \rightarrow 0$ as $T \rightarrow \infty$. In conjunction with (B2), Assumption (B3) imposes a bound on the total number of change-points B , which is permitted to grow slowly with T at a logarithmic rate. Assumption (B4) dictates the minimum requirement on the *cross-sectional size of the change*, for each change-point to be detected as well as being located with accuracy. Note that it is not a trivial matter to gauge the magnitude of a jump in $f_{j,t} = \tilde{g}_{ii',t}$ brought in by the changes in $\Omega_i(t)$ or $\Theta_i(t)$, and hence (B4) is written directly in terms of $\Delta_{j,b}$ rather than using the parameters involved in (1)–(2). Detailed discussion on the high-dimensional efficiency of DC statistic, a tool studied in [Aston and Kirch \(2014\)](#) that allows the quantification and comparison of the power of different change-point tests, can be found in [Cho \(2016\)](#).

Theorem 1. Let $\hat{\eta}_b$, $b = 1, \dots, \hat{B}$ ($1 < \hat{\eta}_1 < \dots < \hat{\eta}_{\hat{B}} < T$) denote the change-points estimated by the DCBS algorithm with a test criterion $\pi_{d,T}$. Assume that (A1)–(A5) and (B1)–(B4) hold and $\pi_{d,T}$ satisfies $C' d \underline{\Delta}_{d,T}^{-1} T^{5(1-\gamma)/2} \log T < \pi_{d,T} < C'' \underline{\Delta}_{d,T} T^{\gamma-1/2}$ for some constants $C', C'' > 0$ and $\varpi > 2\vartheta$ for ϑ in (B3). Then there exists $c_0 > 0$ such that

$$\mathbb{P} \left\{ \hat{B} = B; |\hat{\eta}_b \mathbb{I}(b \leq \hat{B}) - \eta_b| < c_0 \epsilon_T \text{ for } b = 1, \dots, B \right\} \rightarrow 1$$

as $T \rightarrow \infty$, where $\epsilon_T = d \underline{\Delta}_{d,T}^{-2} T^{5(1-\gamma)} \log^{2\varpi} T$.

From the condition imposed on the rate of $\underline{\Delta}_{d,T}$ in (B4), it is easily seen that $\epsilon_T/T^\gamma \rightarrow 0$ as $T \rightarrow \infty$. That is, in the re-scaled time interval $[0, 1]$, the estimated change-points satisfy $T^{-1}|\hat{\eta}_b - \eta_b| \leq T^{-\gamma}|\hat{\eta}_b - \eta_b| \rightarrow 0$ for all $b = 1, \dots, B$. Defining the optimality in change-point detection as when each of the true change-points and the corresponding estimated change-point are within the distance of $O_p(1)$ (see e.g. [Korostelev \(1987\)](#)), it is attained up to a logarithmic factor when the change-points are maximally spread with $\gamma = 1$, $\tilde{\Delta}_b \sim 1$ and $m_b \sim d$, where $a \sim b$ indicates that $a = O(b)$ and $b = O(a)$.

3.3 Choice of parameters for transformation

While Theorem 1 is attained by $x_{j,t}$ resulting from any transformation g_1 meeting (A5), empirical performance of the two-stage methodology is influenced by the choice of the coefficients $C_{i,j}$, $j = 0, \dots, p+q$. As in the references given at the beginning of Section 3.1, we may replace $C_{i,j}$ with the maximum likelihood estimates (MLEs) of the GARCH parameters obtained under the stationarity, say $\hat{\omega}_i, \hat{\alpha}_{i,j}$, $1 \leq j \leq p$ and $\hat{\beta}_{i,k}$, $1 \leq k \leq q$.

The BASTA-res algorithm proposed by [Fryzlewicz and Subba Rao \(2014\)](#) is applied to the transformation of univariate time-varying ARCH process which is formulated similarly to (3). They recommend the use of ‘dampened’ versions of GARCH parameters. In our setting, this leads to the choice of $C_{i,0} = \hat{\omega}_i$, $C_{i,j} = \hat{\alpha}_{i,j}/F_i$, $1 \leq j \leq p$ and $C_{i,p+k} = \hat{\beta}_{i,k}/F_i$, $1 \leq k \leq q$, with within-series dampening parameters $F_i \geq 1$. Empirically, the motivation behind the introduction of F_i is as follows. For $r_{i,t}$ with time-varying parameters, we often observe that $\hat{\alpha}_{i,j}$ and $\hat{\beta}_{i,k}$ are over-estimated such that $\sum_{j=1}^p \hat{\alpha}_{i,j} + \sum_{k=1}^q \hat{\beta}_{i,k}$ is close to, or even exceeds, one, while $\hat{\omega}_i$ is under-estimated. Therefore, using the raw estimates in place of $C_{i,j}$ ’s leads to $U_{i,t}$ where any change in $\mathbb{E}(U_{i,t})$ induced by a change-point in $\Omega_i(t)$ tends to be small. Hence we adopt the dampening parameter F_i which is chosen as

$$F_i = \max \left[1, \frac{\min(0.99, \sum_{j=1}^p \hat{\alpha}_{i,j} + \sum_{k=1}^q \hat{\beta}_{i,k})}{\max \{0.01, 1 - (\sum_{j=1}^p \hat{\alpha}_{i,j} + \sum_{k=1}^q \hat{\beta}_{i,k})\}} \right].$$

By construction, F_i is bounded as $F_i \in [1, 99]$ and brings $\hat{\omega}_i$ and $\sum_{j=1}^p \hat{\alpha}_{i,j} + \sum_{k=1}^q \hat{\beta}_{i,k}$ to approximately the same scale.

Also, g_1 involves the unobservable conditional variance $h_{i,t}$, which we propose to replace

with

$$\widehat{h}_{i,t} = \widehat{\omega}_i + \sum_{j=1}^p \widehat{\alpha}_{i,j} r_{i,t-j}^2 + \sum_{k=1}^q \widehat{\beta}_{i,k} \widehat{h}_{i,t-k}. \quad (9)$$

Typically, the GARCH orders p and q are unknown. We propose to use $(p, q) = (1, 1)$: the GARCH(1, 1) model is very simple yet is known to provide a good fit and accurate predictions for a wide range of datasets (see e.g., [Hansen and Lunde \(2005\)](#)). We also note that our approach allows the additional flexibility to the model with time-varying parameters. In simulation studies reported in Section 4, we study the effect of misspecifying the GARCH orders on change-point analysis, which shows that the choice of $(p, q) = (1, 1)$ works well even when it under-specifies the GARCH orders.

Theoretically, both choices of $s_{i,i'} \in \{1, -1\}$ within g_2 are permitted as any changes in $\mathbb{E}(U_{i,t}^{1/2} U_{i',t}^{1/2})$ are detectable by examining $\mathbb{E}\{(U_{i,t}^{1/2} - s_{i,i'} U_{i',t}^{1/2})^2\}$ with either of $s_{i,i'} \in \{1, -1\}$. However, its choice may influence the empirical performance in the sense that a certain value results in a transformed series which exposes the structural changes better. Based on the observations made in [Cho and Fryzlewicz \(2015\)](#), we favour the choice $s_{i,i'} = \text{sign}(\widehat{\text{corr}}_{s,e}(U_{i,t}^{1/2}, U_{i',t}^{1/2}))$ where $\widehat{\text{corr}}_{s,e}(\cdot, \cdot)$ denotes the sample correlation computed over a segment $[s, e]$.

3.4 Choice of threshold for DCBS algorithm

Theorem 1 provides a range for the rate of $\pi_{d,T}$ that returns consistent estimation of multiple change-points. However, the theoretical range involves typically unattainable knowledge on the quantities such as γ or $\underline{\Delta}_{d,T}$ and even when such knowledge is available, finite sample performance may be affected by the choice of the multiplicative constant to the given rate. Instead, we propose a parametric resampling procedure that enables us to approximate the distribution of $\mathcal{T}_{s,e}$ in the presence of no change-points. A similar approach was adopted in the bootstrap tests proposed by [Kokoszka and Teyssière \(2002\)](#) in the context of testing the presence of a change-point in the parameters of univariate GARCH models.

Bootstrap algorithm for threshold selection.

Step 1: Fit a GARCH(p, q) model to each $\{r_{i,t}\}_{t=1}^T$ and estimate the $p + q + 1$ GARCH parameters for all $i = 1, \dots, N$. As suggested in Section 3.3, we use $p = q = 1$ in our numerical studies.

Step 2: Generate bootstrap samples $\{\boldsymbol{\varepsilon}_t^\ell, 1 \leq t \leq T\}$ of the vector of empirical residuals

$$\widehat{\boldsymbol{\varepsilon}}_t = (\widehat{h}_{1,t}^{-1/2} r_{1,t}, \dots, \widehat{h}_{N,t}^{-1/2} r_{N,t})^\top \text{ (recall (9) for } \widehat{h}_{i,t} \text{) for } \ell = 1, \dots, R.$$

Step 3: Simulate MGARCH series R times, as

$$r_{i,t}^\ell = (h_{i,t}^\ell)^{1/2} \varepsilon_{i,t}^\ell, \quad \text{where} \quad h_{i,t}^\ell = \widehat{\omega}_i + \sum_{j=1}^p \widehat{\alpha}_{i,j} (r_{i,t-j}^\ell)^2 + \sum_{k=1}^q \widehat{\beta}_{i,k} h_{i,t-k}^\ell$$

for $\ell = 1, \dots, R$.

Step 4: From the ℓ th bootstrap realisation $\{r_{i,t}^\ell, 1 \leq i \leq N; 1 \leq t \leq T\}$, we obtain $\mathcal{T}_{s,e}^\ell$ in the same manner as $\mathcal{T}_{s,e}$, with $[s, e]$ denoting an interval that is examined at some iteration of the DCBS algorithm. For a given significance level $\alpha \in [0, 1]$, our choice of $\pi_{d,T}$ is the $100(1 - \alpha)\%$ -quantile of $\mathcal{T}_{s,e}^\ell$, $\ell = 1, \dots, R$.

4 Simulation study

4.1 Models

We study the change-point detection consistency of the two-stage change-point detection methodology described in Section 3 on the datasets simulated from the following models. The choices of parameters for (M0)–(M1) are considered in Fryzlewicz and Subba Rao (2014), while those for (M2)–(M3) are considered in Kokoszka and Teyssière (2002), in the context of *single* change-point test in *univariate* GARCH processes.

(M0) **Stationary MGARCH (1, 1) processes.** Let $\omega_i = \omega + \delta_{\omega,i}$, $\alpha_{i,1} = \alpha + \delta_{\alpha,i}$ and $\beta_{i,1} = \beta + \delta_{\beta,i}$, where $\delta_{\cdot,1} \stackrel{iid}{\sim} \mathcal{U}(-\Delta, \Delta)$ for some small $\Delta > 0$ is added to each GARCH parameter so that every $r_{i,t}$ has a slightly different set of GARCH parameters. The innovations are generated from two different distributions, namely (i) $\boldsymbol{\varepsilon}_t \stackrel{iid}{\sim} \mathcal{N}(\mathbf{0}, \Sigma)$ where $\sigma_{i,i'} = \rho^{|i-i'|}$ with $\rho = -0.75$ and (ii) $\varepsilon_{i,t} \stackrel{iid}{\sim} t_{10}$ for each i and t , and $T = 1000$.

$$(M0.1) \quad (\omega, \alpha_1, \beta_1) = (0.4, 0.1, 0.5).$$

$$(M0.2) \quad (\omega, \alpha_1, \beta_1) = (0.1, 0.1, 0.8).$$

(M1) **tv-MGARCH (1, 1) processes with a single change-point.** Change-points are introduced to GARCH parameters at $\eta_i \in \{[T/2], [0.9T]\}$ as in (1)–(2) with $T = 1000$. For a randomly chosen $i \in \mathcal{S}_1 \subset \{1, \dots, N\}$, GARCH parameters $\omega_i(t), \alpha_{i,1}(t)$ and

$\beta_{i,1}(t)$ for $i \in \mathcal{S}_1$ change at $t = \eta_1$ as $\omega_i(t) = \omega^{(1)}\mathbb{I}(t \leq \eta_1) + \omega^{(2)}\mathbb{I}(t > \eta_1) + \delta_{\omega,i}$, $\alpha_{i,1}(t) = \alpha_1^{(1)}\mathbb{I}(t \leq \eta_1) + \alpha_1^{(2)}\mathbb{I}(t > \eta_1) + \delta_{\alpha,i}$ and $\beta_{i,1}(t) = \beta_1^{(1)}\mathbb{I}(t \leq \eta_1) + \beta_1^{(2)}\mathbb{I}(t > \eta_1) + \delta_{\beta,i}$, where $|\mathcal{S}_1| = \lfloor \varrho N \rfloor$ with $\varrho \in \{1, 0.75, 0.5, 0.25\}$ controlling the ‘sparsity’ of the change-point. Also, $\delta_{\cdot,1} \stackrel{iid}{\sim} \mathcal{U}(-\Delta, \Delta)$ is as in (M0), and $\varepsilon_t \sim \mathcal{N}(\mathbf{0}, \Sigma(t))$ with $\Sigma(t) = \Sigma$ defined in (M0).

$$(M1.1) \quad (\omega, \alpha_1, \beta_1) : (0.4, 0.1, 0.5) \rightarrow (0.4, 0.1, 0.6).$$

$$(M1.2) \quad (\omega, \alpha_1, \beta_1) : (0.4, 0.1, 0.5) \rightarrow (0.4, 0.1, 0.8).$$

$$(M1.3) \quad (\omega, \alpha_1, \beta_1) : (0.1, 0.1, 0.8) \rightarrow (0.1, 0.1, 0.7).$$

$$(M1.4) \quad (\omega, \alpha_1, \beta_1) : (0.1, 0.1, 0.8) \rightarrow (0.1, 0.1, 0.4).$$

$$(M1.5) \quad (\omega, \alpha_1, \beta_1) : (0.4, 0.1, 0.5) \rightarrow (0.5, 0.1, 0.5).$$

$$(M1.6) \quad (\omega, \alpha_1, \beta_1) : (0.4, 0.1, 0.5) \rightarrow (0.8, 0.1, 0.5).$$

$$(M1.7) \quad (\omega, \alpha_1, \beta_1) : (0.1, 0.1, 0.8) \rightarrow (0.3, 0.1, 0.8).$$

$$(M1.8) \quad (\omega, \alpha_1, \beta_1) : (0.1, 0.1, 0.8) \rightarrow (0.5, 0.1, 0.8).$$

(M2) **tv-MGARCH (1, 1) processes with two change-points.** For a randomly chosen $i \in \mathcal{S}_1 \subset \{1, \dots, N\}$, GARCH parameters $\omega_i(t)$, $\alpha_{i,1}(t)$ and $\beta_{i,1}(t)$ change at $\eta_1 = \lfloor T/4 \rfloor$ as below.

$$(M2.1) \quad (\omega, \alpha_1, \beta_1) : (0.1, 0.3, 0.3) \rightarrow (0.15, 0.25, 0.65).$$

$$(M2.2) \quad (\omega, \alpha_1, \beta_1) : (0.1, 0.3, 0.3) \rightarrow (0.125, 0.1, 0.6).$$

$$(M2.3) \quad (\omega, \alpha_1, \beta_1) : (0.1, 0.3, 0.3) \rightarrow (0.15, 0.15, 0.25).$$

Also, a change-point is introduced to the covariance matrix of the innovations at $\eta_2 = \lfloor 3T/5 \rfloor$ as below. Initially, $\varepsilon_t \sim \mathcal{N}(\mathbf{0}, \Sigma(t))$ with $\Sigma(t) = \Sigma$ defined in (M0). For a randomly chosen $i \in \mathcal{S}_2 \subset \{1, \dots, N\}$, rows of $\Sigma(t)$ corresponding to such $\varepsilon_{i,t}$ swap their locations arbitrarily. We set $|\mathcal{S}_1| = |\mathcal{S}_2| = \lfloor \varrho N \rfloor$ with $\varrho \in \{1, 0.75, 0.5, 0.25\}$, and consider the sample size $T = 500$.

(M3) **Misspecification of the orders p and q .**

(M3.1) Over-specification. The two change-points are introduced to tv-MGARCH(1, 1) processes as in (M2.1)–(M2.2) (referred to as (M3.1.1)–(M3.1.2)), but the GARCH orders are misspecified in Stage 1 as $(p, q) = (2, 2)$.

(M3.2) Under-specification. The two change-points are introduced to tv-MGARCh(2, 2) processes as in (M2), with the GARCH parameters change at η_1 as:

$$(M3.2.1) \quad (\omega, \alpha_1, \alpha_2, \beta_1, \beta_2): (0.1, 0.1, 0.2, 0.1, 0.2) \rightarrow (0.15, 0.15, 0.1, 0.35, 0.3); \text{ or}$$

$$(M3.2.2) \quad (\omega, \alpha_1, \alpha_2, \beta_1, \beta_2): (0.1, 0.1, 0.2, 0.1, 0.2) \rightarrow (0.125, 0.1, 0, 0.3, 0.3),$$

and the covariance matrix of the innovations change at η_2 as in (M2). The GARCH orders are misspecified in Stage 1 as $(p, q) = (1, 1)$.

(M4) Full-factor multivariate GARCH(1, 1) model with time-varying factors and loadings. Proposed in [Vrontos et al. \(2003\)](#), each $r_{i,t}$ is generated as a linear combination of the independent *factors* $f_{j,t}$, $j = 1, \dots, N$ which are GARCH(1, 1) processes.

$$\mathbf{r}_t = \mathbf{W}\mathbf{f}_t, \quad \mathbf{f}_t | \mathcal{F}_{t-1} \sim \mathcal{N}_N(\mathbf{0}, \mathbf{H}_t), \quad \mathbf{H}_t = \text{diag}(h_{1,t}, \dots, h_{N,t}),$$

$$\text{where } h_{i,t} = \omega_i + \alpha_{i,1}f_{i,t-1}^2 + \beta_{i,1}h_{i,t-1}, \quad t = 1, \dots, T; \quad i = 1, \dots, N,$$

with $w_{i,i'} \stackrel{iid}{\sim} \mathcal{N}(1, 1)$ for the loading matrix \mathbf{W} . For a randomly chosen $i \in \mathcal{S}_1 \subset \{1, \dots, N\}$, GARCH parameters of \mathbf{f} change at $\eta_1 = [T/4]$ as in (M2.1)–(M2.2) (referred to as (M4.1)–(M4.2)). Another change-point is introduced to the loading matrix at $\eta_2 = [3T/5]$, by swapping the rows of \mathbf{W} corresponding to randomly chosen $i \in \mathcal{S}_2 \subset \{1, \dots, N\}$, which brings in a change in the conditional cross-correlations as well as within-series conditional variance. The cardinality of \mathcal{S}_1 and \mathcal{S}_2 is controlled as in (M2) with $\varrho \in \{1, 0.75, 0.5, 0.25\}$, and we consider $T = 500$.

4.2 Results

Conducting only the first iteration of the binary segmentation procedure in Stage 2 of the proposed methodology, we performed the at-most-one-change test on the data simulated from (M0)–(M1) over 100 realisations, which enables us to investigate its size and power behaviour, respectively, along with accuracy in change-point estimation; see Tables 1–5.

When the innovations are generated from a Gaussian distribution with cross-correlations, the test manages to keep the size below the significance level $\alpha = 0.05$ when $N = 50$, while spurious false alarm is observed when $N = 100$ for (M0.2). We note that, although not directly comparable, Table 1 of [Fryzlewicz and Subba Rao \(2014\)](#) observed similar size behaviour from their BASTA-avg2 as well as the change-point test from [Andreou and Ghysels \(2002\)](#) for *univariate* GARCH processes generated with the same GARCH parameters as in

(M0.2). When the innovations are drawn as i.i.d. random variables from a t_{10} -distribution, the parameter configuration of (M0.2) brings in greater size distortion.

As expected, the test achieves higher power when the change-point is ‘dense’ cross-sectionally (with larger ϱ), and better change-point location accuracy. For most GARCH parameter configurations, the test attains power above 0.9 even when the change-point is relatively sparse ($\varrho = 0.25$), but for (M1.2), (M1.4) and (M1.8). Interestingly, the univariate change-point tests adopted in Table 1 of [Fryzlewicz and Subba Rao \(2014\)](#) for comparative simulation studies, performed uniformly worse for (M1.1) and (M1.5) compared to other models, for which our test performs well. We also note that even when the location of the change-point is skewed ($\eta_1 = [0.9T]$), our method generally attains high power and location accuracy if the change-point is not too sparse, in most settings where it shows good performance when the change-point is centrally located ($\eta_1 = [T/2]$).

Tables 6–9 report the results from applying the proposed methodology to tv-MGARCH processes generated as described in (M2)–(M4), and Figures 1–8 in the supplementary document show the locations of estimated change-points. (M2.1)–(M2.2) bring in a change in the variance of $r_{i,t}$, $i \in \mathcal{S}_1$ at $t = \eta_1$ (with greater change under (M2.1)), while it remains the same in (M2.3), which is reflected in the total number of the estimated change-points as well as the accuracy in locating η_1 under different settings. More specifically, when unconditional variance of $r_{i,t}$ does not vary despite the change in the GARCH parameter, such a change is not well detected in the transformation of \mathbf{r}_t after Stage 1. Between the two types of change-points, the detection of η_1 becomes more challenging when it is sparse cross-sectionally, while η_2 is detected with high accuracy regardless of its sparsity under (M2.2)–(M2.3).

Tables 7–8 indicate that misspecifying the GARCH orders (p, q) does not worsen the performance of our methodology. On the contrary, in the case of (M3.2), under-specification of (p, q) results in improved detection power and location accuracy when the change-points are sparse cross-sectionally, for both the change-point in the GARCH parameters (see (M3.2.2)) and that in the cross-correlations (see (M3.2.1)).

The full-factor MGARCH model in (M4) has been chosen chiefly due to the ease of generating high-dimensional GARCH processes under the model. For (M4.2), the two change-points are detected with accuracy comparable to that observed under (M2)–(M3). The high accuracy is also observed under the model in (M4.1), albeit with over-segmentation due to a third change-point spuriously detected towards the end of the series (see the supplementary document).

Table 1: (M0) Size of the change-point test at $\alpha = 0.05$ when $T = 1000$.

n	Gaussian $\varepsilon_{i,t}$		t_{10} -distributed $\varepsilon_{i,t}$	
	(M0.1)	(M0.2)	(M0.1)	(M0.2)
50	0.01	0.05	0.03	0.13
100	0.02	0.09	0.02	0.3

Table 2: (M1) Power of the change-point test at $\alpha = 0.05$ and the accuracy of $\hat{\eta}_1$ (% of $|\hat{\eta}_1 - \eta_1| < \log^2 T$) when $N = 50$, $T = 1000$ and $\eta_1 = \lceil T/2 \rceil$.

ϱ	(M1.1)		(M1.2)		(M1.3)		(M1.4)	
	power	accuracy (%)						
1	1.00	100	1.00	100	1.00	100	0.96	84
0.75	1.00	100	1.00	100	1.00	100	0.91	79
0.5	1.00	100	1.00	99	1.00	100	0.57	47
0.25	0.96	91	0.83	73	0.99	97	0.12	7
ϱ	(M1.5)		(M1.6)		(M1.7)		(M1.8)	
	power	accuracy (%)						
1	1.00	100	1.00	100	1.00	100	1.00	98
0.75	1.00	100	1.00	100	1.00	100	1.00	98
0.5	1.00	100	1.00	100	1.00	100	0.98	93
0.25	0.99	93	1.00	98	1.00	99	0.54	43

Table 3: (M1) Power of the change-point test at $\alpha = 0.05$ and the accuracy of $\hat{\eta}_1$ when $N = 100$, $T = 1000$ and $\eta_1 = \lceil T/2 \rceil$.

ϱ	(M1.1)		(M1.2)		(M1.3)		(M1.4)	
	power	accuracy (%)						
1	1.00	100	1.00	100	1.00	100	1.00	96
0.75	1.00	100	1.00	100	1.00	100	1.00	93
0.5	1.00	100	1.00	100	1.00	100	0.94	83
0.25	1.00	98	1.00	90	1.00	100	0.46	36
ϱ	(M1.5)		(M1.6)		(M1.7)		(M1.8)	
	power	accuracy (%)						
1	1.00	100	1.00	100	1.00	100	1.00	100
0.75	1.00	100	1.00	100	1.00	100	1.00	100
0.5	1.00	100	1.00	100	1.00	100	1.00	99
0.25	1.00	100	1.00	100	1.00	100	0.98	93

Table 4: (M1) Power of the change-point test at $\alpha = 0.05$ and the accuracy of $\hat{\eta}_1$ (% of $|\hat{\eta}_1 - \eta_1| < \log^2 T$) when $N = 50$, $T = 1000$ and $\eta_1 = [0.9T]$.

ϱ	(M1.1)		(M1.2)		(M1.3)		(M1.4)	
	power	accuracy (%)						
1	1.00	100	1.00	99	1.00	100	0.43	37
0.75	1.00	100	1.00	99	1.00	100	0.27	20
0.5	1.00	100	0.89	84	1.00	100	0.09	6
0.25	0.92	90	0.32	28	0.96	95	0.08	2

ϱ	(M1.5)		(M1.6)		(M1.7)		(M1.8)	
	power	accuracy (%)						
1	1.00	100	1.00	100	1.00	100	0.96	84
0.75	1.00	100	0.99	97	1.00	100	0.89	79
0.5	1.00	100	0.87	86	1.00	100	0.61	50
0.25	0.63	62	0.10	8	1.00	100	0.16	10

Table 5: (M1) Power of the change-point test at $\alpha = 0.05$ and the accuracy of $\hat{\eta}_1$ when $N = 100$, $T = 1000$ and $\eta_1 = [0.9T]$.

ϱ	(M1.1)		(M1.2)		(M1.3)		(M1.4)	
	power	accuracy (%)						
1	1.00	100	1.00	100	1.00	100	0.87	78
0.75	1.00	100	1.00	100	1.00	100	0.65	57
0.5	1.00	100	1.00	100	1.00	100	0.18	15
0.25	1.00	100	0.81	76	1.00	100	0.07	1

ϱ	(M1.5)		(M1.6)		(M1.7)		(M1.8)	
	power	accuracy (%)						
1	1.00	100	1.00	100	1.00	100	1.00	98
0.75	1.00	100	1.00	100	1.00	100	1.00	97
0.5	1.00	100	1.00	100	1.00	100	0.93	84
0.25	1.00	100	0.52	52	1.00	100	0.31	26

Table 6: (M2) The number of estimated change-points (%) and the accuracy in change-point location when $\alpha = 0.05$, $N = 50$ (left), $N = 100$ (right) and $T = 500$.

	ϱ	\hat{B}					accuracy (%)		\hat{B}					accuracy (%)	
		0	1	2	3	≥ 4	η_1	η_2	0	1	2	3	≥ 4	η_1	η_2
(M2.1)	1	0	0	100	0	0	100	100	0	0	100	0	0	100	100
	0.75	0	0	100	0	0	100	100	0	0	100	0	0	100	100
	0.5	0	0	100	0	0	100	100	0	0	100	0	0	100	100
	0.25	0	7	92	1	0	100	93	0	91	9	0	0	100	6
(M2.2)	1	0	0	100	0	0	100	100	0	0	100	0	0	100	100
	0.75	0	2	98	0	0	96	100	0	0	100	0	0	100	100
	0.5	0	38	62	0	0	60	100	0	2	98	0	0	98	100
	0.25	0	95	5	0	0	2	100	0	80	20	0	0	32	84
(M2.3)	1	0	89	11	0	0	3	100	0	68	31	1	0	13	100
	0.75	0	89	11	0	0	3	100	0	85	15	0	0	3	100
	0.5	0	94	6	0	0	0	100	0	88	12	0	0	3	100
	0.25	0	97	3	0	0	0	100	1	96	3	0	0	0	98

Table 7: (M3.1) The number of estimated change-points (%) and the accuracy in change-point location when $\alpha = 0.05$, $N = 50$ (left), $N = 100$ (right) and $T = 500$.

	ϱ	\widehat{B}					accuracy (%)		\widehat{B}					accuracy (%)	
		0	1	2	3	≥ 4	η_1	η_2	0	1	2	3	≥ 4	η_1	η_2
(M3.1.1)	1	0	0	98	2	0	100	100	0	0	100	0	0	100	100
	0.75	0	0	100	0	0	100	100	0	0	99	1	0	100	100
	0.5	0	0	95	5	0	100	100	0	0	100	0	0	100	100
	0.25	0	18	73	8	1	100	80	0	97	3	0	0	100	1
(M3.1.2)	1	0	1	97	2	0	99	100	0	0	99	1	0	100	100
	0.75	0	8	90	2	0	92	100	0	0	99	1	0	100	100
	0.5	0	50	47	3	0	46	100	0	7	85	8	0	93	100
	0.25	1	88	10	1	0	5	99	3	79	18	0	0	27	78

Table 8: (M3.2) The number of estimated change-points (%) and the accuracy in change-point location when $\alpha = 0.05$, $N = 50$ (left), $N = 100$ (right) and $T = 500$.

	ϱ	\widehat{B}					accuracy (%)		\widehat{B}					accuracy (%)	
		0	1	2	3	≥ 4	η_1	η_2	0	1	2	3	≥ 4	η_1	η_2
(M3.2.1)	1	0	0	100	0	0	100	100	0	0	100	0	0	100	100
	0.75	0	0	98	2	0	100	100	0	0	98	2	0	100	100
	0.5	0	0	99	1	0	100	100	0	0	99	1	0	100	100
	0.25	0	5	92	2	1	95	100	0	15	74	11	0	100	83
(M3.2.2)	1	0	0	99	1	0	100	100	0	0	100	0	0	100	100
	0.75	0	0	97	3	0	100	100	0	0	99	1	0	100	100
	0.5	0	0	98	2	0	100	100	0	0	98	2	0	100	100
	0.25	0	45	51	4	0	48	100	0	12	79	9	0	92	93

Table 9: (M4) The number of estimated change-points and the accuracy in change-point location when $\alpha = 0.05$, $N = 50$ (left), $N = 100$ (right) and $T = 500$.

	ϱ	\widehat{B}					accuracy (%)		\widehat{B}					accuracy (%)	
		0	1	2	3	≥ 4	η_1	η_2	0	1	2	3	≥ 4	η_1	η_2
(M4.1)	1	0	5	34	52	9	91	97	0	0	45	44	11	95	97
	0.75	0	3	36	49	12	95	90	0	0	33	60	7	95	96
	0.5	0	4	37	52	7	89	89	0	3	17	64	16	96	88
	0.25	0	14	42	39	5	77	53	0	6	32	48	14	92	70
(M4.2)	1	0	13	87	0	0	87	99	0	4	96	0	0	96	98
	0.75	0	22	78	0	0	79	96	0	7	93	0	0	93	97
	0.5	0	74	24	2	0	29	93	0	38	61	1	0	64	97
	0.25	6	89	5	0	0	8	70	0	93	7	0	0	8	92

5 Real data analysis

In this section, we examine the effect of ignoring possible changes in the volatility of a multi-asset portfolio. We consider Value-at-Risk (VaR), a widely used measure of market risk embraced by financial institutions for regulatory or other internal purposes, which measures the extreme loss (change in value) of an asset or a portfolio of assets with a prescribed probability level during a given holding period. VaR has been criticized due to its unrealistic assumptions (linearity and normality), parameter sensitivity (to estimation and holding periods) and its inadequacy during crises especially when changing correlation between assets is observed (Persaud, 2000; Danielsson, 2002). The last point is of particular interest, since compared to the period of market stability, it is expected that correlations are significantly higher when markets are falling. Jäckel and Rebonato (2001) noted that a risk manager ‘would greatly over-estimate the degree of diversification in his portfolio in the event of a crash if he used the [correlation] matrix estimated during normal periods’. Works to address the VaR critics exist: Valentinyi-Endrész (2004) examined whether detecting and taking into account change-points improves upon VaR forecast. Similarly, Spokoiny (2009) proposed the local change-point analysis to detect regions of volatility homogeneity as an alternative to stationary GARCH modelling, and found that the VaR performed reasonably well.

We propose to examine our method by means of a stressed VaR (sVaR), mainly to highlight the possible flaws of this regulatory proposal to monitor the risks of financial institutions. The Basel Accord (1996 Amendment) requires the use of sVaR which is based on a covariance matrix from a crisis period in the past. The accord does not specify the exact time period to be used but instead proposes the *judgement-based* and the *formulaic* approaches (European Banking Authority, 2012). The former relies on a high-level analysis of the risks related to the holding portfolio, while the latter is a more systematic, quantitative approach. Hence, in addition to a judgement-based approach, information on the stressed past periods will provide a robust risk management, and our proposed methodology can serve as a formulaic approach.

We first introduce the VaR metric which can be formulated as follows:

$$VaR_t(\alpha) = -F^{-1}(\alpha|\mathcal{G}_t),$$

where $F^{-1}(\cdot|\mathcal{G}_t)$ is the quantile function of the loss and profit distribution. This distribution changes over time due to market and portfolio specific conditions, which is embodied in \mathcal{G}_t .

The accuracy of a model to estimate VaR is tested by examining the null hypothesis that the observed probability of occurrence over a specified horizon is equal to the confidence level α , the violation of which signals concerns. Typically, a financial institution should backtest its VaR by means of statistical tests before reporting it to the interested parties, e.g., stakeholders and regulators. [Kupiec \(1995\)](#) proposes two methods, the Proportion of Failure (PoF) and the Time until First Failure (TFF), to accomplish this. For a sample of T observations, the Kupiec test statistics takes the form of likelihood ratio

$$LR_{PoF} = -2 \log \left(\frac{\alpha^{T-x_f} (1-\alpha)^{x_f}}{\left(1 - \frac{x_f}{T}\right)^{T-x_f} \left(\frac{x_f}{T}\right)^{x_f}} \right) \quad \text{and} \quad LR_{TFF} = -2 \log \left(\frac{(1-\alpha)\alpha^{t_f-1}}{\left(\frac{1}{t_f}\right) \left(1 - \frac{1}{t_f}\right)^{t_f-1}} \right),$$

where x_f denotes the number of failures occurred and t_f the number of days until the first failure within the T observations, and α is the VaR level. Under H_0 , both LR_{PoF} and LR_{TFF} are asymptotically χ_1^2 -distributed, and their exceedance of the critical value implies that the VaR model is inadequate. We use these two backtests to examine the performance of our method in the context of stressed VaR.

We collect the daily US Treasury zero-coupon yield curves from the US Federal Reserve Board, which are based on a large set of outstanding bonds and notes with maturity from 1 to 30 years, as well as the daily prices of S&P500 index, see [Figure 1](#). We note that the unconditional correlation between the 30 time series ranges from 0.787 to 0.994. Thirty log-differenced Treasury price series, along with the log-returns of the S&P500 index, from 1 January 2000 to 31 December 2014, serve as an input to our methodology for change-point detection. For validation of our method, we also collect the same data from 1 January 2015 to 31 December 2016.

Our method, using the default parameters described in [Section 3.3](#), gives three change-points as reported in [Table 10](#). We then estimate a DCC model ([Engle, 2002](#)) on each segment defined by two consecutive dates, as well as the sample covariance $\hat{\Sigma}_b$ of the residuals $\hat{\epsilon}_t$ from the fitted DCC models for $1 \leq b \leq 4$, where b denotes the index of the stationary period (patch).

We now take a simple scenario: almost a year (250 days) after the end of the initial sample (i.e., 1 January 2016), a financial institution wishes to report the sVaR of its equally weighted asset portfolio for the year ahead on a daily basis. At the first stage, it calculates the weighted average portfolio returns vector \mathbf{r}_t and its (sample) covariance matrix $\hat{\Sigma}_5$ for the

Period 5 spanning 1 January 2015 to 31 December 2015, which is typically employed in the standard VaR measure. Now, we validate our method by forecasting one-day ahead sVaR using a 250-day rolling window sample. We denote the rolling returns as $\mathbf{r}_{t+\tilde{i}}$ and the rolling (sample) covariance matrix as $\hat{\Sigma}_5^{\tilde{i}}$ for $\tilde{i} = 0, \dots, 250$. Obviously, when $\tilde{i} = 0$ then $\hat{\Sigma}_5^0 := \hat{\Sigma}_5$. The question we try to answer is: how will the portfolio sVaR behave using a covariance matrix from different patches in the past?

To calculate the sVaR, a transformation of the following form (Duffie and Pan, 1997) is applied:

$$\mathbf{r}_{b,t+\tilde{i}} = \mathbf{r}_{t+\tilde{i}} (\mathbf{L}_b \mathbf{L}_{\tilde{i}}^{-1})^T \quad \text{for } b = 1, 2, 3, 4 \quad \text{and } \tilde{i} = 0, \dots, 250, \quad (10)$$

where $\mathbf{r}_{b,t+\tilde{i}}$ is the return vector with covariance matrix $\hat{\Sigma}_b$, \mathbf{L}_b is the Cholesky decomposition of $\hat{\Sigma}_b$ and $\mathbf{L}_{\tilde{i}}$ the Cholesky decomposition of the rolling $\hat{\Sigma}_5^{\tilde{i}}$. At the confidence level $\alpha = 0.95$ and 0.99 , we calculate the rolling empirical quantiles of $\mathbf{r}_{b,t+\tilde{i}}$ in order to calculate the sVaR using the four periods identified by our method, see Figure 2 for $\alpha = 0.99$.

The results in Table 10 indicate that the most stressed VaR (found by calculating the quantiles of $\mathbf{r}_{b,t+\tilde{i}}$ for $\tilde{i} = 0$) was obtained from the period spanning from 11 September 2008 to 26 March 2009, a rather expected outcome given the high volatility that the markets experienced after the bankruptcy of Lehman Brothers in September 2008. We note that this period spans a period of less than 12 months, shorter than the maximum allowed duration by the Basel Accord and thus is a valid choice for an sVaR. It also coincides with the Bank of England's view on the historical periods per region with the worst market moves (Bank of England, 2016). Finally, it is worthwhile to notice that Period 4 exhibits 'high stress' characteristics, but less severe than those from the aftermath of the Lehman Brothers collapse.

Having the stressed periods in hand, we turn to the one-day ahead sVaR forecasting exercise. The PoF and TFF tests are used to statistically evaluate the sVaR outputs. For PoF, the null hypothesis for a 250 day period is 12 and 2 expected violations in sVaR at 95% and 99% levels. An sVaR model will be adequate if it cannot reject the null hypothesis. Similarly, for TFF is 20 and 125 days until the first violation occurs at 95% and 99% level, respectively.

Table 11 summarizes the PoF and TFF results where one can see that the stressed Period 3 gives the smallest number of sVaR violations compared to all other periods both for 1% and 5% sVaR. When opting for reporting the 99% sVaR, Periods 3 and 4 are statistically adequate

in contrast to Periods 1 and 2 (see also Figure 2) whereas, opting for the less ‘conservative’ 95% sVaR, Periods 2 and 4 are statistically adequate. Hence, the choice of the most stressed period boils down to the regulator who will decide the sVaR level.

It should be mentioned that adopting the ‘traffic light’ approach of the Basel Accord (Basle Committee on Banking Supervision, 1996) will reveal Period 3 as the most appropriate input to the sVaR measure at both 95% and 99% levels. According to this approach, a 99% (95%) VaR model is in the green zone and therefore deemed adequate when 0 to 4 (0 to 17) violations occur in a period of 250 days. In the PoF setting, any number of violations fewer than the expected violations is treated similarly with those of more than the expected violations. This is due to the fact that the null hypothesis of the PoF test is two-side.

Table 10: The table reports the three change-points estimated by our methodology (bold) from 1 January 2000 to 31 December 2014, and the corresponding periods of stationarity. It also reports the sVaR obtained for the period spanning from 1 January 2015 to 31 December 2015 using the covariance matrices from the respective periods.

	Period range		sVaR	
	From	Until	95%	99%
Period 1	[01/01/2000	31/12/2007]	-0.01787	-0.02619
Period 2	(31/12/2007	11/09/2008]	-0.02870	-0.04306
Period 3	(11/09/2008	26/03/2009]	-0.05688	-0.08142
Period 4	(26/03/2009	31/12/2014]	-0.03491	-0.04675

Table 11: The table reports the number of sVaR violations using each respective stressed period (above) and the number of days until the first violation (below) in brackets. Low probabilities (in italics) indicate rejection of H_0 , i.e., sVaR measure is not adequate.

PoF				
sVaR	Period 1	Period 2	Period 3	Period 4
99%	<i>0.0000</i> [22]	<i>0.0583</i> [6]	<i>0.2805</i> [1]	<i>0.1596</i> [5]
95%	<i>0.0000</i> [46]	<i>0.1291</i> [18]	<i>0.0043</i> [4]	<i>0.6582</i> [14]

TFF				
sVaR	Period 1	Period 2	Period 3	Period 4
99%	<i>0.0197</i> [3]	<i>0.2099</i> [21]	<i>0.8431</i> [121]	<i>0.2099</i> [21]
95%	<i>0.1230</i> [3]	<i>0.1230</i> [3]	<i>0.9507</i> [21]	<i>0.5204</i> [10]

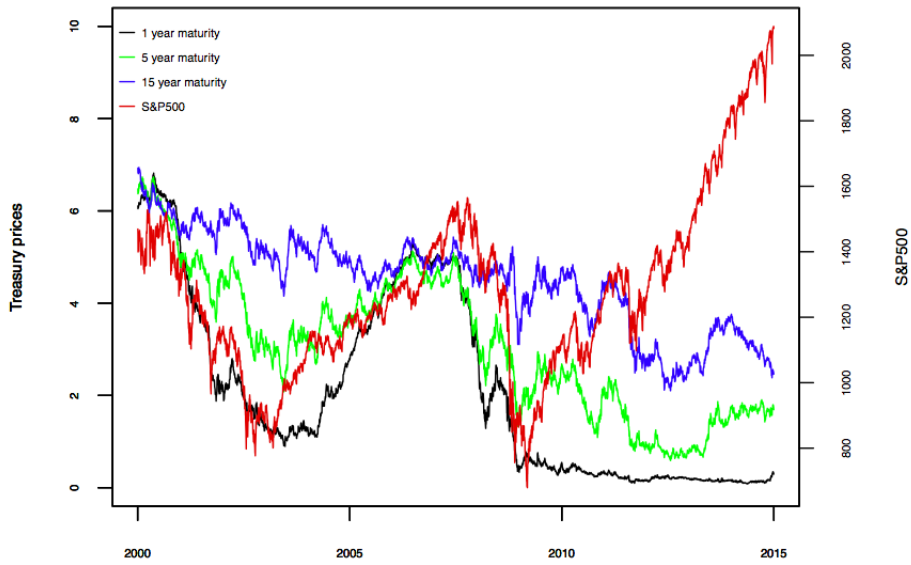


Figure 1: Daily Treasury prices for three different maturities (left axis) and the S&P500 index (right axis).

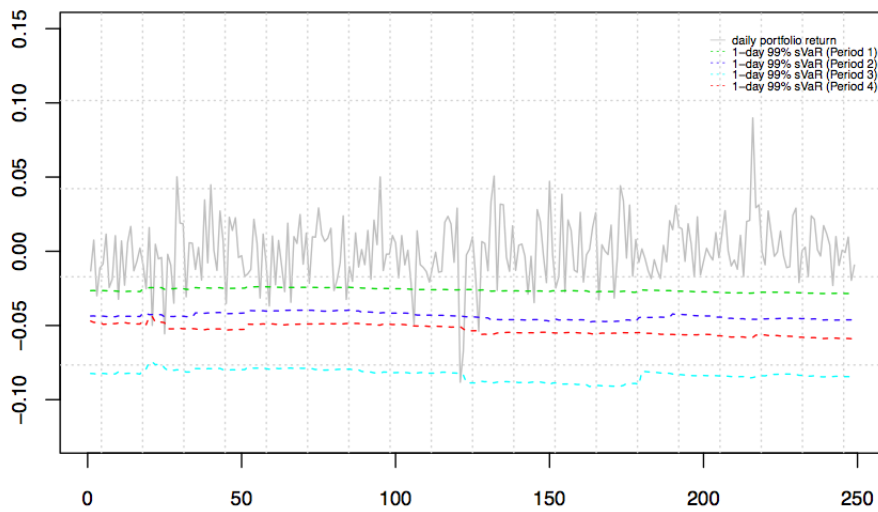


Figure 2: Returns of a portfolio of US Treasury zero-coupon and the S&P500 index (equally weighted) for the testing (rolling) period. The coloured lines indicate the one-day ahead stressed VaR.

6 Conclusions

In this paper, we propose a methodology for detecting multiple change-points in both within-series and cross-correlation structures of multivariate volatility processes. The two-stage methodology first transforms the N -dimensional series so that the structural change-points are detectable as change-points in the means of $N(N + 1)/2$ -dimensional transformed data, which serves as an input to the multiple change-point detection algorithm in the second stage. We show the consistency of the methodology in terms of the total number and locations of estimated change-points, and propose a bootstrap procedure for threshold selection, which shows reasonably good performance in our simulation studies. Finally, we apply the proposed method to demonstrate its usage in identifying periods of ‘stress’ in a multivariate financial dataset consisting of thirty US Treasury zero-coupon yield curves and the S&P500 index. This exercise indicates the efficacy of our methodology in risk management tasks, such as when calculating the (stressed) Value-at-Risk of a portfolio of risky assets.

Acknowledgements

Haeran Cho’s work was supported by the Engineering and Physical Sciences Research Council grant no. EP/N024435/1.

References

- Andreou, E. and E. Ghysels (2002). Detecting multiple breaks in financial market volatility dynamics. *Journal of Applied Econometrics* 17(5), 579–600.
- Andreou, E. and E. Ghysels (2003). Tests for breaks in the conditional co-movements of asset returns. *Statistica Sinica* 13, 1045–1073.
- Aston, J. A. and C. Kirch (2014). Efficiency of change point tests in high dimensional settings. *arXiv preprint, arXiv:1409.1771*.
- Baele, L. (2003). Did emu increase equity market correlations? *Financieel Forum, Bank en Financiewezen* 6, 356–359.
- Baillie, R. T. and Bollerslev, T. (1991). Intra-day and inter-market volatility in foreign exchange rates. *The Review of Economic Studies* 58(3), 565–585.

- Bank of England (2016). *Stress testing the UK banking system: guidance on the traded risk methodology for participating banks and building societies*. <http://www.bankofengland.co.uk/financialstability/Documents/stresstesting/2016/tradedriskguidance.pdf>.
- Basle Committee on Banking Supervision (1996). *Supervisory framework for the use of ‘back-testing’ in conjunction with the internal models approach to market risk capital requirements*. <http://www.bis.org/publ/bcbs22.pdf>.
- Bauwens, L., S. Laurent, and J. V. Rombouts (2006). Multivariate garch models: a survey. *Journal of Applied Econometrics* 21(1), 79–109.
- Berkes, I., L. Horváth, and P. Kokoszka (2004). Testing for parameter constancy in garch(p, q) models. *Statistics and Probability Letters* 70(4), 263–273.
- Bollerslev, T. (1990). Modelling the coherence in short-run nominal exchange rates: a multivariate generalized arch model. *The Review of Economics and Statistics*, 498–505.
- Bollerslev, T., R. F. Engle, and J. M. Wooldridge (1988). A capital asset pricing model with time-varying covariances. *Journal of Political Economy* 96(1), 116–131.
- Boussama, F., F. Fuchs, and R. Stelzer (2011). Stationarity and geometric ergodicity of bekk multivariate garch models. *Stochastic Processes and their Applications* 121, 2331–2360.
- Cappiello, L., R. F. Engle, and K. Sheppard (2006). Asymmetric dynamics in the correlations of global equity and bond returns. *Journal of Financial Econometrics* 4(4), 537–572.
- Cho, H. (2016). Change-point detection in panel data via double cusum statistic. *Electronic Journal of Statistics* 10(2), 2000–2038.
- Cho, H. and P. Fryzlewicz (2015). Multiple change-point detection for high-dimensional time series via sparsified binary segmentation. *Journal of the Royal Statistical Society: Series B* 77(2), 475–507.
- Danielsson, J. (2002). The emperor has no clothes: Limits to risk modelling. *Journal of Banking & Finance* 26(7), 1273–1296.
- De Pooter, M. and D. Van Dijk (2004). Testing for changes in volatility in heteroskedastic time series – a further examination. Technical report, Econometric Institute.

- Diebold, F. and A. Inoue (2001). Long range and regime switching. *Journal of Econometrics* 105(1), 131–159.
- Du, X., L. Y. Cindy, and D. J. Hayes (2011). Speculation and volatility spillover in the crude oil and agricultural commodity markets: A bayesian analysis. *Energy Economics* 33(3), 497–503.
- Duffie, D. and J. Pan (1997). An overview of value at risk. *The Journal of Derivatives* 4(3), 7–49.
- Engle, R. (2002). Dynamic conditional correlation: A simple class of multivariate generalized autoregressive conditional heteroskedasticity models. *Journal of Business & Economic Statistics* 20(3), 339–350.
- Engle, R. F. and K. F. Kroner (1995). Multivariate simultaneous generalized arch. *Econometric Theory* 11(01), 122–150.
- European Banking Authority (2012). *Guidelines on Stressed Value At Risk*. <https://www.eba.europa.eu/documents/10180/104547/EBA-BS-2012-78--GL-on-Stressed-VaR-.pdf>.
- Ewing, B. T. and F. Malik (2013). Volatility transmission between gold and oil futures under structural breaks. *International Review of Economics & Finance* 25, 113–121.
- Fan, J., M. Wang, and Q. Yao (2008). Modelling multivariate volatilities via conditionally uncorrelated components. *Journal of the Royal Statistical Society: Series B* 70(4), 679–702.
- Fryzlewicz, P. and S. Subba Rao (2011). Mixing properties of arch and time-varying arch processes. *Bernoulli* 17(1), 320–346.
- Fryzlewicz, P. and S. Subba Rao (2014). Multiple-change-point detection for auto-regressive conditional heteroscedastic processes. *Journal of the Royal Statistical Society: Series B*, 903–924.
- Groen, J., G. Kapetanios, and S. Price (2013). Multivariate methods for monitoring structural change. *Journal of Applied Econometrics* 28(2), 250–274.
- Hamilton, J. D. (2003). What is an oil shock? *Journal of Econometrics* 113(2), 363–398.
- Hansen, C. S. (2001). The relation between implied and realised volatility in the danish option and equity markets. *Accounting & Finance* 41(3), 197–228.

- Hansen, P. R. and A. Lunde (2005). A forecast comparison of volatility models: does anything beat a garch(1, 1)? *Journal of Applied Econometrics* 20(7), 873–889.
- Horváth, L. and M. Hušková (2012). Change-point detection in panel data. *Journal of Time Series Analysis* 33(4), 631–648.
- Jäckel, P. and R. Rebonato (2001). Valuing american options in the presence of user defined smiles and time-dependent volatility: Scenario analysis, model stress and lower bound pricing applications. *Journal of Risk* 4(1), 35–61.
- Jirak, M. (2015). Uniform change point tests in high dimension. *The Annals of Statistics* 43(6), 2451–2483.
- Kokoszka, P. and R. Leipus (2000). Change-point estimation in arch models. *Bernoulli* 6(3), 513–539.
- Kokoszka, P. and G. Teyssière (2002). Change-point detection in garch models: asymptotic and bootstrap tests. Technical report, Universite Catholique de Louvain.
- Korostelev, A. (1987). On minimax estimation of a discontinuous signal. *Theory of Probability & its Applications* 32(4), 727–730.
- Kupiec, P. H. (1995). Techniques for verifying the accuracy of risk measurement models. *The Journal of Derivatives* 3(2), 73–84.
- Lee, S., Y. Tokutsu, and K. Maekawa (2003). The residual cusum test for the constancy of parameters in garch(1, 1) models. Technical report, Seoul National University.
- Mikosch, T. and C. Stărică (2004). Nonstationarities in financial time series, the long-range dependence, and the igarch effects. *The Review of Economics and Statistics* 86(1), 378–390.
- Persaud, A. (2000). Sending the herd off the cliff edge: the disturbing interaction between herding and market-sensitive risk management practices. *The Journal of Risk Finance* 2(1), 59–65.
- Pesaran, M. H. and A. Timmermann (2007). Selection of estimation window in the presence of breaks. *Journal of Econometrics* 137(1), 134–161.
- Ross, S. A. (1989). Information and volatility: The no-arbitrage martingale approach to timing and resolution irrelevancy. *The Journal of Finance* 44(1), 1–17.

- Spokoiny, V. (2009). Multiscale local change point detection with applications to value-at-risk. *The Annals of Statistics* 37, 1405–1436.
- Stock, J. H. and M. W. Watson (2002). Macroeconomic forecasting using diffusion indexes. *Journal of Business & Economic Statistics* 20(2), 147–162.
- Valentinyi-Endr esz, M. (2004). Structural breaks and financial risk management. Technical report, Magyar Nemzeti Bank (Central Bank of Hungary).
- Van der Weide, R. (2002). Go-garch: a multivariate generalized orthogonal garch model. *Journal of Applied Econometrics* 17(5), 549–564.
- Venkatraman, E. S. (1992). Consistency results in multiple change-point problems. *Technical Report No. 24, Department of Statistics, Stanford University*.
- Vostrikova, L. J. (1981). Detecting ‘disorder’ in multidimensional random processes. *Soviet Doklady Mathematics* 24, 55–59.
- Vrontos, I. D., P. Dellaportas, and D. N. Politis (2003). A full-factor multivariate garch model. *The Econometrics Journal* 6(2), 312–334.